

Barkla Bronwyn (Orcid ID: 0000-0002-4691-8023)

**Single cell-type analysis of cellular lipid remodelling in response to salinity in the epidermal bladder cells of the model halophyte *Mesembryanthemum crystallinum*.**

Running title: Cellular lipid remodelling in a halophyte.

Bronwyn J. Barkla<sup>1\*</sup>, Adriana Garibay-Hernández<sup>2,3</sup>, Michael Melzer<sup>3</sup>, Thusitha W. T.

Rupasinghe<sup>4,5</sup>, Ute Roessner<sup>4,5</sup>

<sup>1</sup>Southern Cross Plant Science, Southern Cross University, Lismore, PO Box 157, NSW, Australia, 2479

<sup>2</sup>Instituto de Biotecnología, UNAM, Cuernavaca, Morelos, México 62210

<sup>3</sup>Leibniz Institute of Plant Genetics and Crop Plant Research, OT Gatersleben, Corrensstraße 3, 06466 Seeland, Germany.

<sup>4</sup>School of BioSciences, University of Melbourne, Parkville, VIC, Australia, 3010

<sup>5</sup>Metabolomics Australia, School of BioSciences, University of Melbourne, Parkville, VIC, Australia, 3010

Corresponding author: Bronwyn Barkla, Southern Cross Plant Science, Southern Cross University, Lismore, PO Box 157, NSW, Australia, 2479. Email - [bronwyn.barkla@scu.edu.au](mailto:bronwyn.barkla@scu.edu.au)

The first two authors contributed equally to the manuscript.

This is the author manuscript accepted for publication and has undergone full peer review but has not been through the copyediting, typesetting, pagination and proofreading process, which may lead to differences between this version and the Version of Record. Please cite this article as doi: [10.1111/pce.13352](https://doi.org/10.1111/pce.13352)

**ABSTRACT**

Salt stress causes dramatic changes in the organization and dynamic properties of membranes, however, little is known about the underlying mechanisms involved. Modified trichomes, known as epidermal bladder cells (EBC), on the leaves and stems of the halophyte *Mesembryanthemum crystallinum* can be successfully exploited as a single-cell-type system to investigate salt-induced changes to cellular lipid composition. In this study alterations in key molecular species from different lipid classes highlighted an increase in phospholipid species, particularly those from phosphatidylcholine (PC) and phosphatidic acid (PA), where the latter is central to the synthesis of membrane lipids. Triacylglycerol (TG) species decreased during salinity, while there was little change in plastidic galactolipids. EBC transcriptomic and proteomic data mining revealed changes in genes and proteins involved in lipid metabolism and the upregulation of transcripts for PIPKIB, PI5PII, PIPKIII, and PLD $\delta$ , suggested the induction of signalling processes mediated by phosphoinositides and PA. TEM and flow cytometry showed the dynamic nature of lipid droplets in these cells under salt stress. Altogether, this work indicates the metabolism of TG might play an important role in EBC response to salinity as either an energy reserve for sodium accumulation and/or driving membrane biosynthesis for EBC expansion.

**Key Words** plant abiotic stress, lipid metabolism, salt tolerance, lipid droplets, trichomes, cell membranes, plastoglobules, lipid signalling, triacylglycerides, membrane remodelling.

## **Introduction**

Halophytes are plants that are adapted to grow and reproduce in saline environments normally toxic or severely inhibitory to salt-sensitive plants (Epstein et al., 1980). They offer an invaluable resource to understand plant salt tolerance, providing answers on how plants have adapted to deal with extreme conditions (Flowers et al 2010). Studies into the molecular mechanisms important for withstanding salinity stress in these plants have been directed primarily to the uptake, movement and sequestration of sodium within the plant, with a focus on the transport proteins, their regulation and the signalling pathways activated (Park et al., 2016). However, salt tolerance is complex and additionally involves changes in primary metabolism required for cellular synthesis of compatible solutes to balance salt accumulation (Krasensky and Jonak 2012), as well as changes to membrane lipids and lipid metabolism to adjust to changing cellular water and ionic status (Okazaki and Saito, 2014).

Transcriptomic, proteomic and metabolomic studies, including lipidomics, have shed some light on the importance of lipids in the response of plants to salt treatment, providing evidence that plant lipid metabolism is responsive to salinity at the gene, protein, and metabolite levels (Natera et al., 2015; Kosova et al., 2013; Fercha et al., 2013;

Veeranagamallaiah et al., 2008). However, these studies have generally focused on salt-sensitive plants.

At present, very little is known about global changes in membrane lipids in halophytes despite evidence for salinity-induced alterations in membrane fluidity, permeability, and stability that change with the degree of salt tolerance of the plant (reviewed in Mansour 2013). This finding suggests that the membrane composition of halophytes may respond differently to that from salt-sensitive plants. These responses likely involve membrane lipid remodelling as has been shown for stress-induced changes in composition of membranes in animals, yeast, bacteria and plants (Hulbert et al., 2010; Sévin and Sauer, 2014; Okazaki and Saito, 2014). Furthermore, as most halophytes accumulate and sequester sodium in the large central vacuole (Barkla et al., 2002; Adams et al., 1998), these strongly ionic conditions would most likely necessitate alterations in the membrane lipid composition, a phenomenon already documented for yeast endomembranes (Schneider et al., 1999). Changes in membrane lipid composition in response to salt-stress can directly affect the structure and activity of proteins embedded in the membranes, triggering signalling cascades (Testerink and Munnik, 2011; Okazaki and Saito, 2014), activating membrane bound transcription factors (Seo et al., 2010), regulating vesicular trafficking (Heilmann and Heilmann, 2012), and altering ion and metabolite fluxes (Gamber and Shapiro, 2007). Specifically, phosphoinositides (phosphorylated phosphatidylinositol species) and phosphatidic acid have been shown to directly affect membrane curvature and charge as well as play a role in recruiting target proteins to particular membranes

influencing their localization and/or activity (Bargmann and Munnik, 2006; Munnik and Vermeer, 2010; Testerink and Munnik, 2011). A universal role of these signalling lipids in plant osmotic stress response has been proposed, having been proven to be responsive to salt treatment (Zonia and Munnik, 2004; Darwish et al., 2009; Bargmann et al., 2009; Meringer et al., 2016; Meijer et al., 2017; Xia et al., 2017). Nevertheless, the majority of these studies have been performed in salt-sensitive photosynthetic organisms.

Recent findings have pointed out that not only membrane polar lipids, but also triacylglycerols (TG) may play an important role in plant stress response. It has been suggested that these neutral glycerolipids are more than a carbon and energy reserve in plant storage tissues, being involved in vegetative tissues in cell division and expansion, stomatal opening, and membrane lipid remodelling (Yang and Benning, 2018). In plants, certain stress conditions have most commonly been linked with TG accumulation, as shown for heat stress, oxidative stress and prolonged darkness (Higashi et al., 2015; Fan et al., 2017). Physiological functions of stress-accumulated TG indicates their importance in storage of chemical energy and materials for membrane lipid biosynthesis and remodelling, transient sequestration of free FA, as well as to production of FA-derived defensive compounds (Shimada et al., 2018; Yang and Benning, 2018), however, a role of TG in salt tolerance has remained understudied.

In the model halophyte, *Mesembryanthemum crystallinum*, sodium accumulation follows a gradient with highest levels measured in the modified trichomes called epidermal

bladders cells (EBC) (Barkla et al., 2002; Adams et al., 1998) that line the stem, leaf and flower bud. These cells are present on the untreated plants from germination but swell significantly in volume once the plants are salt-treated and become highly polyploid (Barkla et al., 2018, unpublished data). EBC offer a unique opportunity to study salinity-induced alterations in a single cell-type system, thus avoiding the use of highly heterogeneous cell populations that are common in total leaf or root tissue analysis, which can lead to averaging of cell-type sample data, therefore obscuring variations within individual cell types, and resulting in false conclusions (Narayanan et al., 2016). These cells offer a direct window on how salt accumulation can affect the cells' lipid profile.

This study builds on our single cell-type-systems biology approach to understand salt tolerance in *M. crystallinum* and more specifically, the development and role of the EBC (Barkla et al., 2012; Oh et al., 2015; Barkla and Vera-Estrella, 2015; Barkla et al., 2016; Barkla et al., 2018). Here, we investigated the lipid composition of EBC using targeted analysis to profile quantitatively the salt-induced alterations in key plant lipid species of different classes. Our results provide new insights into the effect of salinity on lipids from a halophyte and allow us to integrate our accumulating knowledge on the salt-induced changes in transcripts, proteins and metabolites in EBC with the data of cell-specific regulation of lipid metabolism.

## **Materials and methods**

### *Plant material*

*Mesembryanthemum crystallinum* was grown from seeds collected from an inbred line. Potting mix consisted of one third sphagnum peat moss (TEAM Theriault and Hachey, Canada), one-third vermiculite (no. 2, Auspearl, Australia), and one-third perlite (p400, Auspearl, Australia), supplemented with slow release fertilizer (Osmocote 16-9-12, Scotts) and micronutrients (Micromax granular, Scotts), added to 15 cm diameter one litre plastic pots. Plants were grown in a greenhouse under natural irradiation and photoperiod from October 2016 to March 2017. Temperature was maintained through evaporative cooling and during this period fluctuated from a minimum of 15 °C at night, to a maximum of 35 °C, during the hottest days, a temperature range well tolerated by this plant. Adult plants (6 weeks after germination) were either watered daily with tap water or treated with NaCl (200 mM) for 2 weeks.

#### *Isolation of EBC and lipid extraction*

Stem sections were frozen in liquid nitrogen for 5 to 10 min, then removed and allowed to thaw briefly for 1 min. Individual frozen EBC could then be scraped off and immediately collected into a 2 mL Eppendorf tube suspended in a bath of liquid nitrogen. For each biological replicate (six for untreated plants and six for salt-treated plants), 100 EBC were collected. Cells were sonicated for 10 min and an aliquot was taken for total protein determination according to the method of Bradford (Barkla et al., 2002). To each tube of 100 EBC, 1.5 mL of 75% isopropanol with 0.01 % BHT (butylated hydroxytoluene) were added. The samples were incubated at 75 °C for 15 min in a circulating water bath and then snap-

frozen in liquid nitrogen. To thawed samples, 750  $\mu\text{L}$  of chloroform and 300  $\mu\text{L}$  of MilliQ water were added, samples were vortexed and then incubated on a rocking shaker for 1 h. Two mL of 2:1 chloroform:methanol (v/v) were added, samples were vortexed and incubated on a rocking shaker for a further 30 min. Following incubation, 500  $\mu\text{L}$  1 M KCl was added, samples were vortexed and then centrifuged at 3000 rpm for 5 min at 4  $^{\circ}\text{C}$ . The upper phase was discarded by aspiration and 1 mL of MilliQ water was added. The samples were vortexed and centrifuged at 3000 rpm for 5 min at 4  $^{\circ}\text{C}$ . The upper phase was discarded by aspiration and the lower phase was aliquoted into pre-weighed 2 mL HPLC glass vials (Agilent). Samples were vacuum-dried under the following conditions, 500 mbar for 5 min, 450 mbar for 5 min, 400 mbar for 5 min, 350 mbar for 5 min, 300 mbar for 5 min, 250 mbar for 5 min, followed by 1 hr at 200 mbar. Dried samples were weighed and dry weight of the extracted lipids was calculated. Lipids were then resuspended in 200  $\mu\text{L}$  of butanol:methanol 1:1 (v/v) with 10 mM ammonium formate for High Performance Liquid Chromatography-Electrospray Ionization-Tandem Mass Spectrometry (HPLC-ESI-MS/MS) analysis.

#### *Targeted HPLC-ESI-MS/MS lipid analysis*

Phospholipid and neutral glycerolipid analyses were carried out using HPLC-ESI-MS/MS. Lipids were separated by injecting 5  $\mu\text{L}$  aliquots onto a 50 mm  $\times$  2.1 mm  $\times$  2.7  $\mu\text{m}$  Ascentis Express RP Amide column (Supelco, Sigma, St Louis, USA) at 35  $^{\circ}\text{C}$ , using an LC 1200 (Agilent Technologies, Santa Clara, US). Lipids were eluted at 0.2 mL  $\text{min}^{-1}$  over a 5 min gradient of



water/methanol/tetrahydrofuran (50:20:30, v/v/v) to water/methanol/tetrahydrofuran (5:20:75, v/v/v), with the final solution held for 3 min. These lipids were further analysed by ESI-MS/MS using an Agilent 6410 Triple Quadrupole (Agilent Technologies, Santa Clara, US). Glycerolipid species from each class were identified and quantified using multiple reaction monitoring (MRM) in positive mode with a 20 ms dwell time for the simultaneous measurements of ~20 to 50 compounds, and the chromatographic peak width of 30 to 45 sec; the minimum data points collected across the peak were 12 to 16. Optimised parameters for capillary, fragmentor, and collision voltages were 4000, 140-380, and 15–60 V, respectively. In all cases, the collision gas was nitrogen at seven L min<sup>-1</sup>. The HPLC-ESI-MS/MS data was processed using Agilent MassHunter quantitative software (version 6) (Mulgrave, Australia).

Galactolipids were analysed by injecting 10 µL aliquots onto a Porashell EC-C18 (100 mm × 2.1 mm, 2.7 µm (Agilent Technologies, Mulgrave, Australia) at 50 °C, using an LC 1290 (Agilent Technologies, Santa Clara, US), and eluted at 0.4 mL min<sup>-1</sup> over a 10 min gradient. The solvent system consisted of (A) methanol:20 mM ammonium acetate (3:7, v/v) and (B) 2-propanol:methanol:20 mM ammonium acetate (6:3:1, v/v/v). The solvent gradient was linear with starting conditions of 65% B for 2 min, increase to 100% B for 8 min, followed by 100% B for 4 min, and then re-equilibrated to starting conditions in 2 min. Galactolipid species were detected by ESI-MS/MS using Sciex Triple TOF 6600 (Mount Waverley, VIC, 3149, Australia), identified and further quantified using MRM in negative mode. Optimised parameters of gas pressure for all curtain, ion source gas 1 and ion source gas 2 were set to

Author Manuscript

be 45 psi. Declustering potential, ion spray voltage and collision energy were set to -200, -4500, and -45 V, respectively, with the accumulation time of 50 ms. Analyst TF software was used to set up the acquisition method and lipid data was processed using MultiQuant software (Sciex, Toronto, Canada).

The lipid species of the following classes were identified using either precursor or neutral loss scans from 100 to 1200 m/z in positive mode: phosphatidylcholine and lyso phosphatidylcholine ( $[M+H]^+$ , precursors of m/z 184.1), phosphatidylethanolamine ( $[M+H]^+$ , neutral loss of m/z 141), phosphatidylserine ( $[M+H]^+$ , neutral loss of m/z 185), phosphatidylinositol ( $[M+H]^+$ , neutral loss of m/z 279), phosphatidylglycerol ( $[M+NH_4]^+$ , neutral loss of m/z 189), and phosphatidic acid ( $[M+H]^+$ , neutral loss of m/z 115). Neutral glycerolipid species were identified in positive ion mode as ammonium ions  $[M+NH_4]^+$  by using MRM transitions based on the neutral loss of different fatty acid species. Galactolipid species were identified in negative ion mode using the MRM method published by Tarazona et al., 2015.

Detected lipid species were annotated as follows, lipid class (sum of carbon atoms in the two fatty acid chains, sum of double bonds in the fatty acid chains). The MRM transitions and specific parameters for detection and quantitation of each lipid molecular species are described in Supplementary Table 1. The MRM transitions for each lipid species were set up as described previously (Natera et al., 2016; Tarazona et al., 2015).

*Data handling, quantification and statistical analysis*

For lipid data quantification, authentic lipid standards from each lipid class (Avanti Polar Lipids, Alabaster, USA) were prepared by combining equal volumes of individual lipid stock solutions. The standard solution was then diluted to provide a set of calibration solutions ranging in concentration from 0.1 to 10  $\mu\text{M}$ . Calibration curves were constructed by least squares linear regression, fitting reverse phase peak area of the analyte against the concentration of the lipid in the reference standards. The concentration of each lipid species in the extract sample was estimated by using the regression model to convert normalized peak area to lipid concentration. The employed lipid standards and their corresponding response factors are described in Supplementary Table 1. The response factors for galactolipids and neutral lipids were not calculated, owing to the variability within the molar responses of the molecular species comprised in these lipid categories. Therefore, these species were quantified by comparing their relative peak areas between samples.

Due to differences in ionization efficiencies between the analysed lipids and the lack of commercially available standards for all the molecular species, peak area of each lipid species relative to the total amount of extracted lipids in each replicate was used to perform univariate analyses (fold-change analysis, Student's *t*-tests) and multivariate principal component analysis using MetaboAnalyst (v3.4.3., Xia and Wishart, 2016). The data was normalised to median and then log-transformed before performing these analyses. Comparison of significant lipid species detected between control and salt treatment was performed using fold-change analysis of normalised data with a significance of false discovery rate (FDR)-adjusted *t*-test *p*-value < 0.05, and number of biological replicates as

n=6. Quantitative data for the glycerolipid molecular species identified in all replicates is provided in Supplementary Table 1.

#### *Nile red staining and flow cytometry*

One hundred frozen EBC from either untreated or salt-treated plants were thawed and diluted in Galbraith's medium and incubated with Nile red (final concentration,  $1 \mu\text{g mL}^{-1}$ ). Samples were passed through a  $30 \mu\text{m}$  filter to remove cellular debris and incubated in the dark for 10 min at room temperature to allow dye uptake. Nile red stained or unstained control cells were analysed with a Cytoflex flow cytometer using the Blue 488 nm laser with a 585/42 nm bandpass filter. Data was analysed using CytExpert version 2 software.

#### *Transmission electron microscopy*

For ultrastructural examination of  $2 \text{ mm}^2$  leaf and stem sections, combined conventional and microwave-assisted fixation, substitution, resin embedding, sectioning and microscopical analysis was performed as described (Kraner et al., 2017).

#### *Transcriptome and proteome data mining*

Samples used to obtain the EBC transcriptomic and proteomic data that was re-analysed in this study came from six-week-old plants treated for two weeks with 200 mM NaCl. Description of these analyses is provided in the results section.

## Results

LC-MS-based lipidomics has allowed rapid and sensitive profiling, quantification and characterization of plant lipids in complex mixtures (Brügger, 2014). While single cell-type studies have looked at transcriptomics, metabolomics and ionomics in specialized plant cells (Libault and Chen, 2015), single cell-type lipidomics studies have so far been limited to root hairs (Wei et al., 2016), and pollen grains (Ischebeck, 2016). This is despite the greater opportunity in single cell-type analysis to decipher the specific contribution of cellular lipid metabolic and regulatory processes to the physiology of the whole plant.

### Changes to overall lipid composition in EBC from salt-treated plants

The overall protein and lipid composition of the EBC changed significantly under salt treatment (Figure 1 A). While the total amount of lipids per EBC decreased by approximately 20% (Figure 1 A, middle panel), the content of phospholipids (PL) on a per cell basis increased 50% compared to control conditions (Figure 1 A, right panel). These results suggested that EBC lipid species respond differently to salt treatment. To address the complexity of the EBC lipidome, as well as to understand the lipid metabolic and regulatory processes occurring during salt treatment, a single cell-type targeted lipidomics analysis was performed.

### Identification of EBC lipid species

The lipidomic analysis was targeted towards glycerolipids, characterized by having the three-carbon carbohydrate glycerol as a common structural modality. In this work, 162 glycerolipid molecular species, present in all six biological replicates from untreated and salt-treated plants, were identified (Supplementary Table 1). Lipids identified belonged to most major glycerolipid classes (Li-Beisson et al., 2010; Vu et al., 2014), including galactolipids (monogalactosyldiacylglycerol –MGDG-, digalactosyldiacylglycerol –DGDG-), PL (phosphatidylcholine –PC-, phosphatidic acid –PA-, phosphatidylethanolamine –PE-, phosphatidylglycerol –PG-, phosphatidylinositol –PI-, phosphatidylserine –PS-, including the monoacyl molecular species lysoPC –LPC-), and neutral glycerolipids (diacylglycerol –DG-, triacylglycerol –TG-). The anionic sulfur-containing lipid sulfoquinovosyldiacylglycerol (SQDG) could not be detected in this analysis most likely owing to its low abundance. This lipid is the least abundant polar glycerolipid in plastid membranes (Boudière et al., 2014). Nevertheless, in agreement with the presence of photosynthetically active chloroplasts in EBC (Barkla et al., 2016), and the identification of the major characteristic plastidic glycerolipids (MGDG and DGDG), SQDG must be present in EBC chloroplasts along with PG to maintain the proper function of photosynthetic membranes (Boudière et al., 2014).

Analysis of the specific contribution of every lipid class to the total amount of measured glycerolipids was only possible for PL (Figure 1 B). We were unable to calculate the response factors for either galactolipids or neutral lipids, owing to the variability within the molar responses of the molecular species comprised in these lipid categories. Not surprisingly, when comparing the proportions within PL classes, PC was the most abundant

(~35%). The next most abundant PL class was PG (~25%), followed by PE, PI, and PA (~10 to 15%); the least abundant classes were PS and LPC (~0.5%) (Figure 1 B). Glycerolipid profiles are highly diverse, as in addition to their primary classification according to the head group, the type and position of the hydrophobic fatty acyl groups (fatty acids –FA–) attached to the glycerol backbone adds a further level of complexity (Nakamura, 2017). A detailed survey of the lipid molecular species comprised within each glycerolipid category identified in EBC is given in this work (Figures 2 and 3, Supplementary Figure 1 and Supplementary Table 1). While the positional distribution of the FA on the glycerolipid moieties cannot be determined from the lipidomic analysis performed in this study, it is possible to predict their FA composition when the overall FA profile is available. Data mining of our EBC-specific GC-TOF-MS-based metabolomics study (Barkla and Vera-Estrella, 2015), together with the analysis of the monoacyl PC (LPC) species identified in EBC (Supplementary Figure 1 and Supplementary Table 1), support the following EBC FA profile (described as number of carbons:number of unsaturations): 9:0, 10:0, 14:0, 16:0, 18:0, 18:1, 18:2, 18:3, 20:0, and 28:0. In *M. crystallinum* leaves, 16:1-cis and 16:1-trans FA have also been identified (Nouairi et al., 2006). Higher plants synthesize glycerolipids through two distinct pathways. The ‘prokaryotic pathway’ refers to glycerolipids exclusively produced within the plastid, which can be distinguished by the presence of 16-carbon FA at the *sn*-2 position of the glycerol backbone. The ‘eukaryotic pathway’ refers to glycerolipids initially synthesized at the endoplasmic reticulum (ER), transferred from the ER to the plastid, and further modified within the plastid; eukaryotic lipids are distinguished by the presence of 18-carbon FA at the

*sn*-2 position (Li-Beisson et al., 2010). Our data suggests that the eukaryotic pathway is very active in EBC, as typical chloroplast lipid classes (MGDG and DGDG) comprise 36-carbon-containing molecular species that likely contain two 18-carbon FA attached to their glycerol backbone; moreover, DGDG species with more than 36-carbons from the two acyl moieties were also identified (Figures 3 A and Supplementary Figure 1).

### **Changes in abundance of EBC glycerolipid species with salt treatment**

Salt-treatment resulted in alterations in the glycerolipid composition of the EBC. The overall amounts of PC, PI, PA, and LPC, were significantly increased on a per cell basis (Figure 1 C), therefore contributing to the higher amount of total PL in EBC during salt treatment (Figure 1 A, right panel). In contrast, total amounts of only two glycerolipid classes, PS and TG, were decreased in salt-treated EBC (Figure 1 C). As PS is one of the less abundant glycerolipids, the lowered amount of TG was mostly responsible for the decrease observed in the total lipid content of salt-treated EBC, which could not be compensated by the increased amounts of PL. Analysis of the data relative to the total lipid weight (Figure 1 D) provided a different perspective. Although the TG content per EBC was decreased by 24% (Figure 1 C), its overall contribution to the lipid fraction remained unchanged (Figure 1 D), suggesting that the proportion of neutral lipids relative to the total lipid content remained constant under salt treatment. In contrast, the contributions of PA, PI, PC, LPC, and PS classes to the total lipid content were still significant under salt treatment. Moreover, the contribution of



PG to the total lipid content was also significantly increased in salt-treated conditions, despite being unchanged on a per cell basis.

To address the specific contributions of the identified lipid molecular species to these changes, a quantitative analysis on normalised data was performed using MetaboAnalyst v3.4.3. (Xia and Wishart, 2016). Principal component analysis presented an unbiased assessment of the data variance structure. Supplementary Figure 2 A shows the scores plot for the dataset of EBC lipid species isolated from untreated and salt-treated plants for the first two principal components. As can be observed, there is separation of the samples into two distinct groups in agreement with the treatment conditions. The first principal component (PC1) explained the greatest variance (31.2%) across the data and separated the samples based on treatment. The second principal component (PC2) separated the components based on sample replicates and accounted for 10.8% of the variance. The specific weight with which each glycerolipid molecular species contributed to the first two principal components is visualized in the loadings plot (Supplementary Figure 2 B).

In total, 34 lipid molecular species were identified as significantly changed in abundance (FDR-adjusted  $p$ -value < 0.05), from which 28 complied with a fold-change threshold higher than two (Supplementary Figure 3 and Supplementary Table 2). In agreement with the changes observed in the EBC glycerolipid content, the lipid molecular species for PC, PA, PG, and PI generally increased, while molecular species for PS and TG generally decreased upon salt treatment (Figures 2 and 3). No PE lipid species, out of a total

of 16 detected, showed alterations in response to salinity treatment (Supplementary Figure 1). All the statistically responsive PL compounds, except PI 36:3, PC 34:2, and PC 34:4, showed at least a two-fold change during salt treatment (Supplementary Figure 3 and Supplementary Table 2). An overall increase was observed in the abundance of 34, 36, and 38-carbon-containing PL molecular species, except for PS 38:3 and PS 38:4, which were the lipid species that mostly contributed to the decreased content of PS in salt-treated EBC (Figure 2D). The 34, 36, and 38 glycerolipid molecular species are most likely comprised by 16/18, 18/18, and 18/20 FA, respectively. An 18-carbon FA length is common to these lipid species, suggesting that their increased amounts are due to a major incorporation of 18-carbon FA into membrane glycerolipids during salt treatment. This is supported by the increased abundance of LPC 18:1, which despite not being statistically significant following data normalisation, clearly contributed to a higher LPC content (Supplementary Figure 1 B), and strongly influenced the discrimination between control and salt-treatment conditions (Supplementary Figure 2 B). An overall increase in 18-carbon containing lipid species is also suggested by the higher levels of MGDG 36:1, which was the only chloroplast-specific glycerolipid responsive to salt, among the 22 identified galactolipid species (Figures 3A and Supplementary Figure 1). The 36:1 glycerolipid species, likely comprising 18:0/18:1 FA, were also increased in PC and PG (Figures 2A and C); PG 36:1 showed the highest increase among all the salt-responsive lipid species (Figure 2C and Supplementary Table 2).

Changes in several lipid molecular species were common to different PL classes. In particular, 34:1 and 36:3 lipids were increased in PA, PC, PG, and PI. Moreover, out of the 17

identified PA molecular species, the six salt-responsive species were also increased in at least one other PL class (Figure 2). Our data therefore suggests that synthesis of membrane PL (PC, PG, PI) from PA, which is their common precursor, is enhanced in EBC from salt-treated *M. crystallinum*.

Neutral glycerolipids, primarily TG species, also changed in salt-treated EBC. The four statistically responsive TG species were decreased in EBC under salt treatment (Figure 3 C), despite the overall TG content per total lipids was not changed (Figure 1 D). Among these, TG 50:3 and TG 52:4 changed more than two-fold (Supplementary Figure 3 and Supplementary Table 2). Therefore, the decrease observed in TG on a per cell basis (Figure 1 C), can be attributed to these molecular species. A single DG species, DG 36:0, was also responsive to salt treatment (Figure 3 B).

### **Lipid droplets are present in the EBC and show salinity-induced alterations**

In plants, neutral TG lipids are packaged and stored into discrete compartments called lipid droplets (LD). While the presence and role of LD in seeds as energy store are well characterised, their location and function in non-seed vegetative tissue are less well known (Murphy 2012; Lersten et al., 2006). In plants, LD can be formed in at least two subcellular locations, the endoplasmic reticulum (ER) and the chloroplast. Lipid droplets in chloroplasts are also referred to as plastoglobules (Pyc et al., 2017). LD are highly dynamic with roles in membrane lipid biosynthesis, stomatal regulation, stress response, pathogen resistance, and

hormone metabolism (Chapman et al., 2012; McLachlan et al., 2016). In *M. crystallinum*, TG species were abundant in the EBC and decreased significantly with salt treatment (Figure 3 C). As TG are highly hydrophobic species, their identification in EBC suggested that they must be localized to LD. Representative electron microscopy images showed the presence of LD in both the chloroplast (plastoglobules) and cytoplasm of the EBC from leaves and stems of control and salt-treated plants (Figure 4). EBC chloroplasts showed the presence of electron-dense plastoglobules (Figures 4 A, C, E, G), while larger LD were detected in the cytoplasm of these cells (Figures 4 B, D, F, H). Ultrastructural analysis showed no significant differences in number and size of plastoglobules in EBC chloroplasts from leaves of control and salt-treated plants (Figures 4 A, B, C, E, G). This pattern is comparable for LD in the cytoplasm of EBC from the leaf (Figures 4 B and F). In contrast, significant differences could be observed in LD in the cytoplasm of EBC from the stem. Here, many more and often bigger LD could be detected in control tissue compared to salt-treated tissue (Figures 4 D and H). While qualitative analysis suggested more LD in the EBC from the stems of control plants compared to salt-treated plants, a quantitative analysis is required to support this. Isolated EBC taken from the stem (100 cells per sample) were stained with Nile red (9-diethylamino-5H-benzo[ $\alpha$ ]phenoxazine-5-one), a lipid-soluble dye, highly fluorescent in non-polar hydrophobic environments, and an excellent probe for the detection of neutral lipids (Satpati and Pal, 2015). Indirect quantification of Nile red fluorescence in EBC by flow cytometry showed that the occurrence of LD in discrete populations in EBC from untreated plants compared to salt-treated plants was greater, as observed from representative dot

plots and flow histograms (Figures 5 A and B). This result agrees with the decreased TG content on a per cell basis observed in EBC from salt-treated plants (Figure 1 C).

### **EBC transcriptomic and proteomic data mining supports a salt-responsive lipid metabolism**

The reference transcriptome for *M. crystallinum*'s EBC (Oh et al., 2015) was surveyed for lipid metabolism-related transcripts. All contigs showing a BLASTN hit (e-value <  $10^{-5}$ ) with an Arabidopsis gene model (TAIR10) were analysed. This represented 38.9% of the total reference transcriptome (37341 non-redundant contigs). *M. crystallinum*'s EBC transcripts associated to acyl-lipid metabolism in the Arabidopsis Acyl-Lipid Metabolism (ARALIP) database (Li-Beisson et al., 2010) were assigned as lipid metabolism-related in this work and classified into different acyl-lipid metabolism pathways. According to this procedure, 528 transcripts (1.4% of the total reference transcriptome) were lipid-metabolism related and could be classified into 18 different lipid pathways (Figure 6 A and Supplementary Table 3). More than 50% of these transcripts are contained within five pathways: FA and wax biosynthesis, PL signalling, oxylipin metabolism, TG and FA degradation, and eukaryotic PL synthesis and editing.

Twenty four percent of the 528 lipid-related EBC transcripts were responsive to salt treatment, from which 56 were statistically up-regulated, whereas 74 were down-regulated ( $p$ -value < 0.01, after Benjamini-Hochberg FDR correction). Comparison of the lipid

pathways to which these responsive transcripts are related (Figure 6 B and Supplementary Table 3) identified a large number involved in FA elongation and wax biosynthesis. In this pathway, 12.5% of the up-regulated genes are involved in cutin metabolism, while 16.2% of the down-regulated ones are related to suberin metabolism. This suggested that modulation of cell wall composition is important under salinity stress in the EBC.

Lipid signalling in EBCs is also highly responsive to salt treatment, as PL signalling genes were mostly up-regulated (Figure 6 B and Supplementary Table 3). Induction of PL-based signalling in salt-treated EBC was not surprising, as it is known to play a role in mediating osmotic stress responses in photosynthetic organisms (Munnik and Vermeer, 2010). Transcriptomic data mining provided insights into the salt-responsive PL-based signalling mechanisms in EBC. Activation of phosphoinositide (PIP) signalling was suggested by the upregulation of gene homologs involved in their direct synthesis (PI-Phosphate Kinase type IB –PIPKIB-; Phosphoinositide 5-Phosphatase type II -PI5P II-; PI-Phosphate Kinase type III –PIPK III-) (Supplementary Table 3). Salt-responsive PA-signalling also likely plays a role due to the statistically differential expression of gene homologs required for PA biosynthesis in plants during osmotic stress (Bargmann and Munnik, 2006; Munnik and Vermeer, 2010; Testerink and Munnik, 2011): PI-specific phospholipase C (PI-PLC), DG kinase (DGK), phospholipase D alpha 1 (PLD $\alpha$ 1) and delta (PLD $\delta$ ) (Supplementary Table 3).

Transcripts for genes in the FA biosynthesis pathway were induced in EBC from salt-treated plants (Figure 6 B) suggesting that FA may be incorporated into newly synthesized

glycerolipids, or channelled into the synthesis of cell wall components. Moreover, APETALA1, a transcription factor known to regulate FA biosynthesis in Arabidopsis (Han et al., 2012), showed a 100 log<sub>2</sub> fold-increase in salt-treated EBC compared to untreated EBC (Supplementary Table 3).

The changes observed in genes related to TG metabolism highlight the dynamic regulation of the neutral lipid content in EBC under salt treatment conditions (Figures 3 C and D). This is supported by the responsiveness of an oleosin gene, whose protein product is a plant LD-specific component important for their stabilization, formation and turnover (Pyc et al., 2017). Comparison of up- and down-regulated TG-related genes indicates a preference for TG degradation rather than for TG biosynthesis in EBC from salt-treated plants (Figure 6 B and Supplementary Table 3).

The EBC proteome was previously analysed through a label free GeLC-MS/MS approach by Barkla et al. (2016). The proteome comprised 438 proteins (35733 spectra, 0.5% decoy FDR), from EBC of either control or salt-treated plants, identified with not less than two unique peptides by applying protein and peptide score-thresholds of 99 and 95 percent, respectively. To get more insights into the EBC lipid metabolism in response to salt treatment, the EBC proteome was surveyed for lipid-related proteins. For this purpose, EBC protein sequences were subjected to a BLASTP analysis against the Arabidopsis TAIR10 annotation to retrieve the corresponding Arabidopsis homologs (e-value < 10<sup>-3</sup>). Then, *M. crystallinum*'s proteins, whose corresponding Arabidopsis homologs have been associated

to the acyl-lipid metabolism in the ARALIP database (Li-Beisson et al., 2010), were assigned as lipid metabolism-related in this work. Using this approach, only four EBC proteins were identified as lipid metabolism-related, lipoxygenase (LOX), PLD $\alpha$ , acyl-CoA oxidase (ACX), and caleosin (Supplementary Table 4). This low number may be attributed to the use of total cellular protein extraction methodology with no fractionation, resulting in a very complex and high dynamic range of proteins, and the relatively low abundance of proteins involved in lipid metabolism. Nevertheless, these four proteins correspond to major lipid pathways that were shown to be salt-responsive in the analysis of the transcriptome: oxylipin metabolism, PL signalling, and TG metabolism, respectively (Supplementary Table 3). These proteins did not show significant changes (Student's *t*-test *p*-value < 0.05), however, the transcripts corresponding to LOX and PLD $\alpha$  were down-regulated under salt treatment compared to control conditions. In addition, the identified caleosin is a homolog of Arabidopsis AtCLO4, a LD-associated calcium-binding protein expressed in non-seed tissues, shown previously to be down-regulated after salt stress (Kim et al., 2011). The presence of this protein in the EBC, together with the identification of oleosin-responsive transcripts, support a role for LD in EBC mediating *M. crystallinum*'s salt tolerance.

## Discussion

In the context of building an integrated picture of the cellular and metabolic processes within the EBC to understand the role of this specialized cell in plant salt tolerance, we have



previously carried out transcriptomic, proteomic, metabolomic and ionic analysis (Barkla et al., 2016; Barkla and Vera-Estrella, 2015; Oh et al., 2015). The EBC from *M. crystallinum* provides a unique single cell-type system to understand salt tolerance and the specific role of modified trichomes. In this study, we focus on EBC lipids to investigate the dynamic changes in cellular lipid composition, brought about in response to salinity stress.

### **Changes in EBC PL support increased membrane lipid synthesis and suggest modulation of PC levels as an adaptive advantage to salt treatment**

Salt treatment resulted in large and significant increases in EBC PL (Figure 1 A, right panel). The increased overall amounts of membrane PL (PC, PG, and PI) and its common precursor (PA), together with the fact that all salt-responsive PA molecular species were also increased in at least one other membrane PL class (Figure 2), strongly support that membrane PL biosynthesis from PA is enhanced in salt-treated EBC, despite their overall lipid content is decreased (Figure 1 A, middle panel). A strong demand for increased synthesis of membranes may be necessary to maintain cell growth, as EBC enlarge in response to salt stress (Oh et al., 2015). Higher PL contents may also be involved in major membrane rearrangements and remodelling events in EBC to modulate membrane fluidity and osmotic balance during salt treatment. Among the increased PL, multiple PC species specifically showed significant up-regulation (Figure 2 A). PC is the most abundant PL in plants and important for membrane structure and function, and changes in amount of this lipid are thought to be involved in adaptive response to abiotic stresses (Tasseva et al., 2004). Salt-

induced increases in total PC in other salt-tolerant plants have been documented: in roots of *Plantago* (Elkahoui et al., 2004; Erdei et al., 1980), in barley (Natera et al., 2016), and in callus cultures of the halophyte *Spartina patens* (Wu et al., 2005). In contrast, salt-sensitive plants appear to show a decrease in PC lipid amounts as was observed in oat and in wheat (Magdy et al., 1994; Norberg and Liljenberg 1991), suggesting that the ability to maintain or increase PC amounts under salt-stress is an adaptive advantage.

### **LD and neutral glycerolipids decrease in salt-treated EBC**

LD and plastoglobules have been documented in the cells of glandular trichomes (Valkama et al., 2004; Turner et al., 2000); however, their presence in non-glandular trichomes or modified trichomes has not been reported. This absence of plastoglobules may reflect the general absence of chloroplasts in the majority of plant trichomes (Laterre et al., 2017). Our studies have shown that EBC contain functioning chloroplasts (Barkla et al., 2016; Figure 4) and chloroplast-specific glycerolipids (MGDG and DGDG) were identified in this work (Figures 3 A and Supplementary Figure 1). Both MGDG and DGDG levels remain unchanged in the EBC following salt treatment (Figures 1 C and D), however, abiotic stress, including salinity, drought, osmotic, heavy metal or freezing stress, commonly results in a decline in MGDG and/or DGDG in non-salt tolerant species (Monteiro de Paula et al., 1993; Gigon et al., 2004; Djebali, 2005; Moellering et al., 2010; Bejaoui et al., 2016). Reduced levels of these chloroplastic lipids have been shown to result in decreased amounts of chlorophyll and changes to chloroplast ultrastructure, ultimately affecting photosynthesis (Dörmann and

Benning, 2002). Stable MGDG and DGDG levels in the EBC chloroplast may represent a salt tolerance response and contribute to the ability of the plant to maintain an optimal efficiency of photosynthesis under salt-stress.

In this work, the presence of plastoglobules and LD in the EBC was confirmed by TEM analysis (Figure 4), and the presence of caleosin, identified in the proteome of the EBC and oleosin-responsive transcripts (Supplementary Tables 3 and 4; Barkla et al., 2016; Oh et al., 2015). Caleosins are major LD proteins that have both structural and functional roles. They have been shown to be involved in the process of lipid degradation (Chapman et al., 2012) and evidence shows they are stress-responsive (Aubert et al., 2010; Kim et al., 2011).

Neutral glycerolipids, in particular TG, were highly salt-responsive in the EBC showing a marked decrease (Figures 1 C and 3 C). These changes in TG quantified by LC-MS were associated with a reduction in abundance of a Nile red fluorescence population attributed to neutral lipids detected by flow cytometry (Figure 5). This was also supported by a decrease in number and size of cytosolic LD in salt-treated EBC, suggested by TEM analysis (Figure 4). Evidence from analysis of the transcriptome also indicated that transcripts for genes involved in TG catabolism are preferentially enriched (Figure 6 B), and a glycerol-3-phosphate acyltransferase GPAT9 homolog, shown to be essential for TG biosynthesis (Schockey et al., 2016; Singer et al., 2016), was downregulated in salt-treated plants (Supplementary Table 3). Altogether, these results suggest that salt treatment promotes degradation of TG comprised in the LD of EBC. This physiological response is contrary to the increased TG abundance typically reported for plant vegetative tissues under stress

conditions (Yang and Benning, 2018), suggesting that decreased TG upon salt treatment may be also an adaptive feature of *M. crystallinum* to salt tolerance. The overall decrease in the lipid content of salt-treated EBC (Figure 1 A, middle panel) can be therefore attributed to the lowered amount of TG, which could not be compensated for by the increased content of PL in salt-treated EBC.

TG metabolism in the EBC may be important for energy supply to drive membrane transport processes required for sodium accumulation. TG lipids are energy dense, storing more than twice the energy as in carbohydrates or proteins (Xu and Shanklin, 2016). In *Arabidopsis* guard cells, there is evidence that TG, present in LD, decrease in the presence of light. Breakdown of TG via oxidation produces ATP required to energize transport processes required for stomatal opening. TG catabolism mutants show delayed light-induced stomatal opening, have reduced LD numbers and decreased H<sup>+</sup>-ATPase activity (McLachlan et al., 2016).

### **TG catabolism and *de novo* lipid biosynthesis may contribute to higher membrane PL levels in EBC during salt treatment**

Metabolic cross-talk between essential membrane lipids and neutral storage lipids has been documented (Bates, 2016; Péter et al., 2017), and is thought to play an important role in stress tolerance (Yang and Benning, 2018). An increased demand for membrane components to sustain EBC expansion during salt treatment would provide a link between the increased PL and decreased TG amounts observed in this study. Increased PL

biosynthesis may be driven by hydrolysis of TG to generate DG and FA, which can then be used as precursors for membrane PL synthesis. The released FA could also provide a source for oxylipin production, as leaf oil bodies have been proposed as subcellular factories for their synthesis (Shimada and Hara-Nishimura, 2015). This is supported by the high amount of oxylipin-related transcripts in EBC, which were highly responsive to salinity (Figure 6 B).

In addition to neutral lipid recycling, *de novo* FA synthesis may also contribute to the increased demand of membrane PL in salt-treated EBC as suggested by the high proportion of up-regulated FA synthesis-related transcripts (Figure 6 B). This is also supported by the increased abundance of 34:1 molecular species within the PA, PC, PG and PI lipid classes (Figure 2), as these molecular species are likely comprising 16/18:1 FA, which are the predominant products from *de novo* FA biosynthesis in the plastid (Koo et al., 2004; Li-Beisson et al., 2010). This agrees with the overall increase of 18:1-containing species within the glycerolipid profile of salt-treated EBC, suggested by the higher abundance of unsaturated 34, 36, and 38 glycerolipid molecular features and the response showed by LPC 18:1 (Supplementary Figure 1).

*De novo* synthesized and/or TG-derived FA would then be immediately incorporated into glycerol-3-phosphate for *de novo* synthesis of PA, a common precursor for the production of membrane glycerolipids that was increased in salt-treated EBC (Figure 1). Alternatively, these FA would be incorporated directly into PC through an acyl editing mechanism followed by their exchange and incorporation into other glycerolipid species (Bates et al., 2007; Bates, 2016). Increased PA could also be derived from PC through the

action of PLD enzymes (Bates, 2016), as their transcripts in EBC were responsive to salt treatment (Supplementary Table 3). A representative diagram for this hypothesis is provided in Figure 7.

**PL-based signalling mechanisms are responsive to salt treatment in EBC from *M. crystallinum***

The results from transcriptomic data mining strongly suggest the induction of PL-signalling mechanisms in salt-treated EBC. As described in Supplementary Figure 4, the upregulation of PIPKIB, PI5P2, and PIPK3, suggest the induction of signalling processes mediated by PI(4,5)P2 and PI(3,5)P2 (phosphatidylinositol 4,5-bisphosphate and 3,5-bisphosphate, respectively), which were not measured in this work as their analysis requires specialized methods (Pettitt et al. 2006). Induction of PIP-signalling pathways in salt-treated EBC is not surprising, as the increased formation of PIP under hyperosmotic conditions has been proposed as a universal response to osmotic stress in photosynthetic organisms (Munnik and Vermeer, 2010). Current evidence supports a role of PI(4,5)P2 and PI(3,5)P2 in multiple membrane-trafficking routes (König et al., 2008; Whitley et al., 2009; Hirano et al., 2017). Accordingly, PIP-signalling may be involved in enhanced membrane trafficking during salinity, as suggested by the increased amounts of membrane PL (Figure 1 A, right panel). A link between PIP-signalling and LD dynamics in salt-treated EBC may also occur, as has been demonstrated for yeast (Ren et al., 2014), and suggested in green microalgae (Garibay-Hernández et al., 2017) and Arabidopsis (Brocard et al., 2017).

In addition to PIP, PA is also believed to act as a lipid second messenger in photosynthetic organisms during various stress responses, and PA production via PLC/DKG and PLD is increased during hyperosmotic stress (Testerink and Munnik, 2011). While most of the components involved in PA-signalling were identified in the EBC transcriptome, the majority of the transcripts in the PLC/DGK pathway were down-regulated with salt treatment (Supplementary Figure 4 and Supplemental Table 3). This suggests that EBC PA production and salt-responsive signalling would be only specifically induced through activation of PLD $\delta$ , as PLD $\alpha$ 1 transcription was also decreased.

### **Acknowledgements**

We thank Timothy R. Rhodes for technical help with the collection of EBC, Alicia Hidden for greenhouse technical support and Kirsten Hoffie (IPK Gatersleben) for support in ultrathin sectioning. This work was supported by a Southern Cross University seed grant to BB. Lipidomics analysis was carried out at Metabolomics Australia which is supported by funds from the Australian Government's National Collaborative Research Infrastructure Scheme (NCRIS) administered through Bioplatforms Australia (BPA) Ltd.

**COMPETING INTERESTING STATEMENT** The authors declare no competing financial interests.

## References

- Adams P., Nelson D.E., Yamada S., Chmara W., Jensen R.G., Bohnert H.J. & Griffiths H. (1998) Growth and development of *Mesembryanthemum crystallinum* (Aizoaceae). *New Phytologist* 138, 171-190.
- Aubert Y., Vile D., Pervent M., Aldon D., Ranty B., Simonneau T., Vavasasseur A. & Galaud J.P. (2010) RD20, a stress-inducible caleosin, participates in stomatal control, transpiration and drought tolerance in *Arabidopsis thaliana*. *Plant and Cell Physiology* 51, 1975-987.
- Bargmann B.O. & Munnik T. (2006) The role of phospholipase D in plant stress responses. *Current Opinion in Plant Biology* 9, 515-522.
- Bargmann B.O.R, Laxalt A.M., ter Riet B., van Schooten B., Merquiol E., Testerink C., Haring M.A., Bartels D. & Munnik T. (2009) Multiple PLDs required for high salinity and water deficit tolerance in plants. *Plant and Cell Physiology* 50, 78-89.
- Barkla B.J., Vera-Estrella R., Camacho-Emiterio J. & Pantoja O. (2002) Na<sup>+</sup>/H<sup>+</sup> exchange in the halophyte *Mesembryanthemum crystallinum* is associated with cellular sites of Na<sup>+</sup> storage. *Functional Plant Biology* 29, 1017-1024.
- Barkla B.J., Vera-Estrella R. & Pantoja O. (2012) Protein profiling of epidermal bladder cells from the halophyte *Mesembryanthemum crystallinum*. *Proteomics* 12, 2862-2865.
- Barkla B.J., Vera-Estrella R. & Raymond C. (2016) Single-cell-type quantitative proteomic and ionomic analysis of epidermal bladder cells from the halophyte model plant



*Mesembryanthemum crystallinum* to identify salt-responsive proteins. *BMC Plant Biology* 16,110.

Barkla B.J. & Vera-Estrella R. (2015) Single cell-type comparative metabolomics of epidermal bladder cells from the halophyte *Mesembryanthemum crystallinum*. *Frontiers in Plant Science*, 6, 435.

Bates P.D., Ohlrogge J.B. & Pollard M. (2007) Incorporation of newly synthesized fatty acids into cytosolic glycerolipids in pea leaves occurs via acyl editing. *Journal of Biological Chemistry* 282: 31206-31216.

Bates P.D. (2016) Understanding the control of acyl flux through the lipid metabolic network of plant oil biosynthesis. *Biochimica et Biophysica Acta - Molecular and Cell Biology of Lipids* 1861, 1214-1225.

Bejaoui F., Salas J.J., Nouairi I., Smaoui A., Abdelly C., Martínez-Force E. & Youssef N.B. (2016) Changes in chloroplast lipid contents and chloroplast ultrastructure in *Sulla carnosa* and *Sulla coronaria* leaves under salt stress. *Journal of Plant Physiology* 198: 32-38.

Boudière L., Michaud M., Petroutsos D., Rébeillé F., Falconet D., Bastien O., ..., Maréchal E. (2014) Glycerolipids in photosynthesis: composition, synthesis and trafficking. *Biochimica et Biophysica Acta - Bioenergetics* 1837: 470-80.

Brocard L., Immel F., Coulon D., Esnay N., Tuphile K., Pascal S., Claverol S., Fouillen L., Bessoule J.J. & Brehelin C. (2017) Proteomic analysis of lipid droplets from

Arabidopsis aging leaves brings new insight into their biogenesis and functions  
*Frontiers in Plant Science* 8, 894.

Brügger B. (2014) Lipidomics, analysis of the lipid composition of cells and subcellular organelles by electrospray ionization mass spectrometry. *Annual Review of Biochemistry* 83, 79-98.

Chapman K.D., Dyer J.M. & Mullen R.T. (2012) Biogenesis and functions of lipid droplets in plants *Journal of Lipid Research*. 53, 215-226.

Darwish E., Testerink C., Khalil M., El-Shihy O. & Munnik T. (2009) Phospholipid signaling responses in salt-stressed rice leaves *Plant and Cell Physiology* 50, 986-997.

Djebali W., Zarrouk M., Brouquisse R., Kahoui E.S., Limam F., Ghorbel M.H. & Chaïbi W. (2005) Ultrastructure and lipid alterations induced by cadmium in tomato (*Lycopersicon esculentum*) chloroplast membranes *Plant Biology* 7,358–368.

Dörmann P. & Benning C. (2002) Galactolipids rule in seed plants. *Trends in Plant Science* 7, 112-117.

Epstein E., Norylon J.D. & Rush DW, (1980) Crops for saline agriculture, a genetic approach. *Science* 210, 399–404.

Fercha A., Capriotti A.L., Caruso G., Cavaliere C., Gherroucha H., Samperi R., Stampachiacchiere S. & Lagana A. (2013) Gel-free proteomics reveal potential biomarkers of priming-induced salt tolerance in durum wheat. *Journal of Proteomics* 91, 486-499.

- Flowers T.J., Galal H.K. & Bromham L. (2010) Evolution of halophytes, multiple origins of salt tolerance in land plants. *Functional Plant Biology* 37, 604–612.
- Gamber N. & Shapiro M.S. (2007) Regulation of ion transport by membrane phosphoinositides. *Nature Review Neuroscience* 8, 921-934.
- Garibay-Hernández A., Barkla B.J., Vera-Estrella R., Martinez A. & Pantoja O. (2017) Membrane proteomic insights into the physiology and taxonomy of an oleaginous green microalga. *Plant Physiology* 173, 390-416.
- Gigon A., Matos A.R., Laffray D., Zuily-Fodil Y. & Pham-Thi A.T. (2004) Effect of drought stress on lipid metabolism in the leaves of *Arabidopsis thaliana* (ecotype Columbia). *Annals of Botany* 94, 345–351.
- Heilmann M. & Heilmann I. (2012) Arranged marriage in lipid signalling? The limited choice of PtdIns(4,5)P<sub>2</sub> in finding the right partner. *Plant Biology* 15, 789-797.
- Higashi Y., Okazaki Y., Myouga F., Shinozaki K. & Saito K. (2015) Landscape of the lipidome and transcriptome under heat stress in *Arabidopsis thaliana*. *Scientific Reports* 5, 10533.
- Hirano T., Munnik T. & Sato M.H. (2017) Inhibition of phosphatidylinositol 3,5-bisphosphate production has pleiotropic effects on various membrane trafficking routes in *Arabidopsis*. *Plant and Cell Physiology* 58: 120-129
- Hulbert A.J. (2010) Metabolism and longevity, is there a role for membrane fatty acids. *Integrative and Comparative Biology* 50, 808-817.

- Ischebeck T. (2016) Lipids in pollen – They are different. *Biochimica and Biophysica Acta - Molecular and Cell Biology of Lipids* 1861, 1315-1328.
- Kim Y.Y., Jung K.W., Yoo K.S., Jeung J.U. & Shin JS (2011) A stress-responsive caleosin-like protein, AtCLO4, acts as a negative regulator of ABA responses in Arabidopsis. *Plant and Cell Physiology* 52, 874–884.
- König S., Ischebeck T., Lerche J., Stenzel I. & Heilmann I. (2008) Salt-stress-induced association of phosphatidylinositol 4,5-bisphosphate with clathrin-coated vesicles in plants. *Biochemical Journal* 415, 387-399.
- Koo A.J.K., Ohlrogge J.B. & Pollard M (2004) On the export of fatty acids from the chloroplast. *Journal of Biological Chemistry* 279, 16101-16110.
- Kosová K., Práil I.T. & Vítámvás P. (2013) Protein contribution to plant salinity response and tolerance acquisition. *International Journal of Molecular Science* 14, 6757-89.
- Kraner M., Link K., Melzer M., Ekici A.B., Uebe S., Tarazona Corrales P., Feussner I. & Sonnewald U. (2017) Choline transporter-like1 (CHER1) is crucial for plasmodesmata maturation in *Arabidopsis thaliana*. *Plant Journal* 89, 394-406.
- Krasensky J. & Jonak C. (2012) Drought, salt, and temperature stress-induced metabolic rearrangements and regulatory networks. *Journal of Experimental Botany* 63,1593-1608.
- Laterre R., Pottier M., Remacle C. & Boutry M. (2017) Photosynthetic trichomes contain a specific Rubisco with a modified pH-dependent activity. *Plant Physiology* 173, 2110-2120.

- Lersten N.R., Czapinski A.R., Curtis J.D., Freckmann R. & Horner H.T. (2006) Oil bodies in leaf mesophyll cells of angiosperms: overview and a selected survey. *American Journal of Botany* 93,1731–1739.
- Li-Beisson Y., Shorrosh B., Beisson F., Andersson M.X., Arondel V, Bates P.D., ..., Durrett T.P. Acyl-lipid metabolism. *Arabidopsis Book*. 2010;8:e0133.
- Libault M. & Chen S. (2015) Plant single cell type systems biology. *Frontiers in Plant Science* 7,35.
- Mansour M.M.F. (2013) Plasma membrane permeability as an indicator of salt tolerance in plants. *Biologia Plantarum* 57, 1-10.
- McLachlan D.H., Lan J., Geilfus C.-M., Dodd A.N., Larson T., Baker A., ..., Hetherington A.M. (2016) The breakdown of stored triacylglycerols is required during light-induced stomatal opening. *Current Biology* 26, 707–712.
- Meijer H.J.G., van Himbergen J.A.J., Musgrave A. & Munnik T. (2017) Acclimation to salt modifies the activation of several osmotic stress-activated lipid signalling pathways in *Chlamydomonas*. *Phytochemistry* 135, 64-72.
- Meringer M.V., Villasuso A.L., Margutti M.P., Usorach J., Pasquare S.J., Giusto N.M., Machado E.E. & Racagni G.E. (2016) Saline and osmotic stresses stimulate PLD/diacylglycerol kinase activities and increase the level of phosphatidic acid and proline in barley roots. *Environmental and Experimental Botany* 128, 69-78.
- Moellering E.R., Muthan B. & Benning C. (2010) Freezing tolerance in plants requires lipid remodeling at the outer chloroplast membrane. *Science* 330, 226–228.

- Monteiro de Paula F., Pham Thi A.T., Zuily Fodil Y., Ferrari-Iliou R., Vieira da Silva J. & Mazliak P. (1993) Effect of water stress on the biosynthesis and degradation of polyunsaturated lipid molecular species in leaves of *Vigna unguiculata*. *Plant Physiology and Biochemistry* 31, 707–715.
- Munnik T. & Vermeer J.E.M. (2010) Osmotic stress-induced phosphoinositide and inositol phosphate signalling in plants. *Plant Cell and Environment* 33, 655-669.
- Murphy D.J. (2012) The dynamic roles of intracellular lipid droplets, from archaea to mammals. *Protoplasma*, 249, 541-585.
- Nakamura Y. (2017) Plant phospholipid diversity: emerging functions in metabolism and protein-lipid interactions. *Trends in Plant Science* 22:1027-1040.
- Narayanan M., Martins A.J. & Tsang J.S. (2016) Robust inference of cell-to-cell expression variations from single- and k-cell profiling. *PLoS Computer Biology* 12, e1005016.
- Natera S.H.A., Hill C.B., Rupasinghe T.W.T. & Roessner U. (2016) Salt-stress induced alterations in the root lipidome of two barley genotypes with contrasting responses to salinity. *Functional Plant Biology* 43, 207-219.
- Nouairi I., Ghnaya T., Ben Youssef N., Zarrouk M. & Habib Ghorbel M (2006) Changes in content and fatty acid profiles of total lipids of two halophytes: *Sesuvium portulacastrum* and *Mesembryanthemum crystallinum* under cadmium stress. *Journal of Plant Physiology* 163: 1198-1202.

- Oh D.-H., Barkla B.J., Vera-Estrella R., Pantoja O., Lee S.-Y., Bohnert H.J. & Dassanayake, M. (2015) Cell type-specific responses to salinity - the epidermal bladder cell transcriptome of *Mesembryanthemum crystallinum*. *New Phytologist* 207, 627-644.
- Okazaki Y. & Saito K. (2014) Roles of lipids as signalling molecules and mitigators during stress response in plants. *Plant Journal* 79, 584-596.
- Péter M., Glatz A., Gudmann P., Gombos I, Török Z., Horváth I, Vigh L. & Balough G. (2017) Metabolic crosstalk between membrane and storage lipids facilitates heat stress management in *Schizosaccharomyces pombe*. *PLoS ONE* 12, e0173739.
- Pettitt T.R., Dove S.K., Lubben A., Calaminus S.D.J. & Wakelam M.J.O. (2006) Analysis of intact phosphoinositides in biological samples. *Journal of Lipid Research* 47, 1588-1596.
- Pyc M., Cai Y., Greer M.S., Yurchenko O., Chapman K.D., Dyer J.M. & Mullen R.T. (2017) Turning over a new leaf in lipid droplet biology. *Trends in Plant Science* 22, 597-607.
- Ren J., Pei-Chen L.C., Pathak M.C., Temple B.R., Nile A.H., Mousley C.J., ..., Bankaitis V.A. (2014) A phosphatidylinositol transfer protein integrates phosphoinositide signaling with lipid droplet metabolism to regulate a developmental program of nutrient stress-induced membrane biogenesis. *Molecular Biology of the Cell* 25, 712-727.
- Satpati G.G. & Pal R. (2015) Rapid detection of neutral lipid in green microalgae by flow cytometry in combination with Nile red staining—an improved technique. *Annals of Microbiology* 65, 937-949.

- Schneiter R., Brugger B., Sandhoff R., Zellnig G., Leber A., Lampl M., Athenstaedt K., Hrastik C., Eder S., Daum G., Paltauf F., Wieland F.T. & Kohlwein S.D. (1999) Electrospray ionization tandem mass spectrometry (ESI-MS/MS) analysis of the lipid molecular species composition of yeast subcellular membranes reveals acyl chain-based sorting/remodelling of distinct molecular species en route to plasma membrane. *Journal of Cell Biology* 146, 741-754.
- Seo P.J., Kim M.J., Song J.S., Kim Y.S., Kim H.J. & Park C.M. (2010) Proteolytic processing of an Arabidopsis membrane-bound NAC transcription factor is triggered by cold-induced changes in membrane fluidity. *Biochemical Journal* 427,359–367.
- Sévin D.C., Stählin J.N., Pollak G.R., Kuehne A. & Sauer U. (2016) Global metabolic responses to salt stress in fifteen species. *PLoS ONE* 11, e0148888.
- Shimada T.L. & Hara-Nishimura I. (2015) Leaf oil bodies are subcellular factories producing antifungal oxylipins. *Current Opinion in Plant Biology* 25, 145-150.
- Shimada T.L., Hayashi M. & Hara-Nishimura I. (2018) Membrane dynamics and multiple functions of oil bodies in seeds and leaves. *Plant Physiology* 176, 199-207.
- Tarazona P., Feussner K., Feussner I. (2015) An enhanced plant lipidomics method based on multiplexed liquid chromatography-mass spectrometry reveals additional insights into cold- and drought-induced membrane remodeling. *Plant Journal* 84, 621-33.
- Tasseva G., Richard L. & Zackowski A. (2004) Regulation of phosphatidylcholine biosynthesis under salt stress involves choline kinases in *Arabidopsis thaliana*. *FEBS Letters* 566, 115-120.



- Testerink C. & Munnik T. (2011) Molecular, cellular and physiological responses to phosphatidic acid formation in plants. *Journal of Experimental Botany* 62, 2349-2361.
- Turner G.W., Gershenzon J. & Croteau R.B. (2000) Development of peltate glandular trichomes of peppermint. *Plant Physiology* 124, 665-680.
- Veeranagamallaiah G., Jyothsnakumari G., Thippeswamy M., Reddy P.C.O., Surabhi G.-K., Sriranganayakulu G., ..., Sudhakar C. (2008) Proteomic analysis of salt stress responses in foxtail millet (*Setaria italica* L. cv. Prasad) seedlings. *Plant Science* 175, 631-641.
- Vu H.S., Shiva S., Roth M.R., Tamura P., Zheng L., Li M., ..., Welti R. (2014) Lipid changes after leaf wounding in *Arabidopsis thaliana*, expanded lipidomic data form the basis for lipid co-occurrence analysis. *Plant Journal* 80, 728-743.
- Wei F., Fanella B., Guo L. & Wang X. (2016) Membrane glycerolipidome of soybean root hairs and its reponse to nitrogen and phosphate availability. *Scientific Reports* 6, 36172.
- Whitley P., Hinz S. & Doughty J. (2009) Arabidopsis FAB1/PIKfyve proteins are essential for development of viable pollen. *Plant Physiology* 151, 1812-1822.
- Xia J. & Wishart D.S. (2016) Using MetaboAnalyst 3.0 for comprehensive metabolomics data analysis. *Current Protocols in Bioinformatics* 55, 14.10.1-14.10.91.
- Xia K.K., Wang B., Zhang J.W., Li Y., Yang H.L. & Ren D.T. (2017) Arabidopsis phosphoinositide-specific phospholipase C 4 negatively regulates seedling salt tolerance. *Plant Cell and Environment* 40, 1317-1331.

- Xu C. & Shanklin J. (2016) Triacylglycerol metabolism, function, and accumulation in plant vegetative tissues. *Annual Review of Plant Biology* 67,179–206.
- Yang Y. & Benning C. (2018) Functions of triacylglycerols during plant development and stress. *Current Opinion in Biotechnology* 49, 191-198.
- Zonia L. & Munnik T. (2004) Osmotically induced cell swelling versus cell shrinking elicits specific changes in phospholipid signals in tobacco pollen tubes. *Plant Physiology* 134, 813-823.

## Figure Legends

**Figure 1.** Changes in total glycerolipids (phospholipids, galactolipids, neutral glycerolipids) in EBC as a function of salinity treatment. (A) Protein concentration, lipid weight per cell and total phospholipids in EBC from control and salt-treated *M. crystallinum*. Boxes indicate the lower, median and upper quartiles. Whiskers extend from the 5th to 95th percentiles. (B) Changes in the amount of every phospholipid class relative to total phospholipids. (C) Changes in the total amount of glycerolipid classes expressed on a per cell basis. (D) Changes relative to the total weight of analyzed lipids. The amounts of phospholipids are reported as pmoles based on the corresponding response factors of internal lipid standards (Supplementary Table 1). The quantities of galactolipids and neutral glycerolipids are reported as peak area owing to the variation in the molar response within compounds of the same class. Data are mean  $\pm$  standard error of the mean (SEM) of six biological replicates. The significance of differences between control and salt-treated samples was determined through unpaired two-tailed Student's *t*-tests. Statistically significant changes ( $p$ -value  $< 0.05$ ) are indicated with asterisks.

**Figure 2.** Abundance of phospholipid molecular species in EBC from untreated (light grey) and salt-treated (dark grey) *M. crystallinum* plants. Values are mean  $\pm$  SEM of six biological replicates. Asterisks indicate statistically salt-responsive lipid species (FDR-adjusted *t*-test  $p$ -value  $< 0.05$ ) according to the univariate analysis of targeted lipidomics data.

**Figure 3.** Abundance of the galactolipid MGDG and neutral glycerolipids (DG, TG) molecular species in EBC from untreated (light grey) and salt-treated (dark grey) *M. crystallinum* plants. Values are mean  $\pm$  SEM of six biological replicates. Asterisks indicate statistically salt-responsive lipid species (FDR-adjusted *t*-test *p*-value < 0.05) according to the univariate analysis of targeted lipidomics data.

**Figure 4.** Transmission electron microscopy of EBC from leaves and stems of *M. crystallinum*. Ultrastructural analysis of control (A-D) and salt-treated plants (E-H). Chloroplasts with plastoglobules (A, C, E, G) and cytoplasm with lipid droplets (B, D, F, H). M, mitochondria; LD, lipid droplet; P, plastoglobule; V, vacuole. Space bars = 500 nm.

**Figure 5.** Flow cytometry analysis of Nile red stained LD to detect neutral lipids in EBC from control and salt-treated plants. (A) Two-parameter histogram density Dot Plot displaying chlorophyll fluorescence on the x-axis (PerCP-A) and Nile red (FITC-A) on the y-axis. Nile red stained LD excited in the fluorescein isothiocyanate (FITC-A) channel have a yellow gold fluorescence emission that can be clearly distinguished from the background autofluorescence. (B) Data plotted on a single-parameter histogram (FITC-A). Debris and autofluorescence were excluded from the analysis by gating (red ellipse in A). Left hand side – untreated EBC, and right hand side – salt-treated EBC.

**Figure 6.** Classification, relative abundance and salt regulation of lipid metabolism-related transcripts in EBC. (A) EBC transcripts were classified into different acyl-lipid metabolism pathways according to their Arabidopsis homologs in the ARALIP database. The number of

transcripts related to a specific pathway is indicated as a percentage relative to the total of EBC lipid metabolism-related transcripts (528). (B) Quantitative analysis and distribution in acyl-lipid metabolism pathways of statistically salt-responsive transcripts in EBC. The number of transcripts related to a specific acyl-lipid metabolism pathway is indicated as a percentage relative to the total of up- (56) or down-regulated (74) transcripts, respectively.

**Figure 7.** TG catabolism and *de novo* FA biosynthesis may contribute to higher membrane PL in EBC during salinity. In this model we propose that an increase in FA synthesized *de novo* and exported from the plastid (1), as well as FA derived from the hydrolysis of TG contained in the LD (2), both contribute to a pool of activated FA (acyl-CoA) for the increased production of membrane phospholipids. These FA can be either directly incorporated into G3P (3) for *de novo* synthesis of PA, or channeled into PC through an acyl-editing mechanism (4). PA can also be produced by the activity of PLD on PC (5). An augmented pool of PA may support an increased synthesis of membrane PL (6). In addition to membrane PL synthesis and/or remodelling (6), the FA derived from TG catabolism may also be involved in oxylipin metabolism and/or play a role as source of energy and carbon building blocks in salt-treated EBC. The changes in the overall amounts of glycerolipid classes on a per cell basis are indicated: upward red arrow, increase; downward blue arrow, decrease.

**Supporting information**

**Supplementary Table 1.** Glycerolipid molecular species identified in the EBC of *M. crystallinum* under control and salt-treated conditions. Values represent the peak area under the chromatogram normalized per total weight of analyzed lipids in every replicate. Multiple reaction monitoring (MRM) transitions and specific parameters for the quantitation and identification of lipid molecular species are provided, as well as the authentic lipid standards used in this work. The response factors for these standards are also indicated.

**Supplementary Table 2.** Lipid molecular species identified as statistically significant from the volcano plot with a threshold of  $p < 0.05$  for FDR-adjusted  $t$ -test  $p$ -values. FC- fold-change (salt treatment relative to control); FDR-false discovery rate.

**Supplementary Table 3.** Lipid metabolism-related transcripts identified in the *M. crystallinum* EBC transcriptome. EBC transcripts associated to acyl-lipid metabolism (ARALIP) database (Li-Beisson et al., 2010) were assigned as lipid metabolism-related in this work (528 transcripts, 1.4 % of the total reference transcriptome) and classified into different pathways (18).

**Supplementary Table 4.** Lipid metabolism-related proteins identified in the *M. crystallinum* EBC proteome. EBC proteins whose Arabidopsis homologues are associated to the acyl-lipid metabolism (ARALIP) database (Li-Beisson et al., 2010) were assigned as lipid metabolism-related in this work.

**Supplementary Figure 1.** Abundance of the galactolipid, DGDG, and the PL, PE and LPC, molecular species in EBC from untreated (light grey) and salt-treated (dark grey) *M. crystallinum* plants. Values are mean  $\pm$  SEM of six biological replicates. None of the lipid species showed statistically significant changes.

**Supplementary Figure 2.** (A) Principal component analysis (PCA) scores plot (x-axis, first component, y-axis, second component) of control (pink) and salt-treated (green) EBC lipid species. Symbol numbers represent different biological replicates. Colored ellipses are used

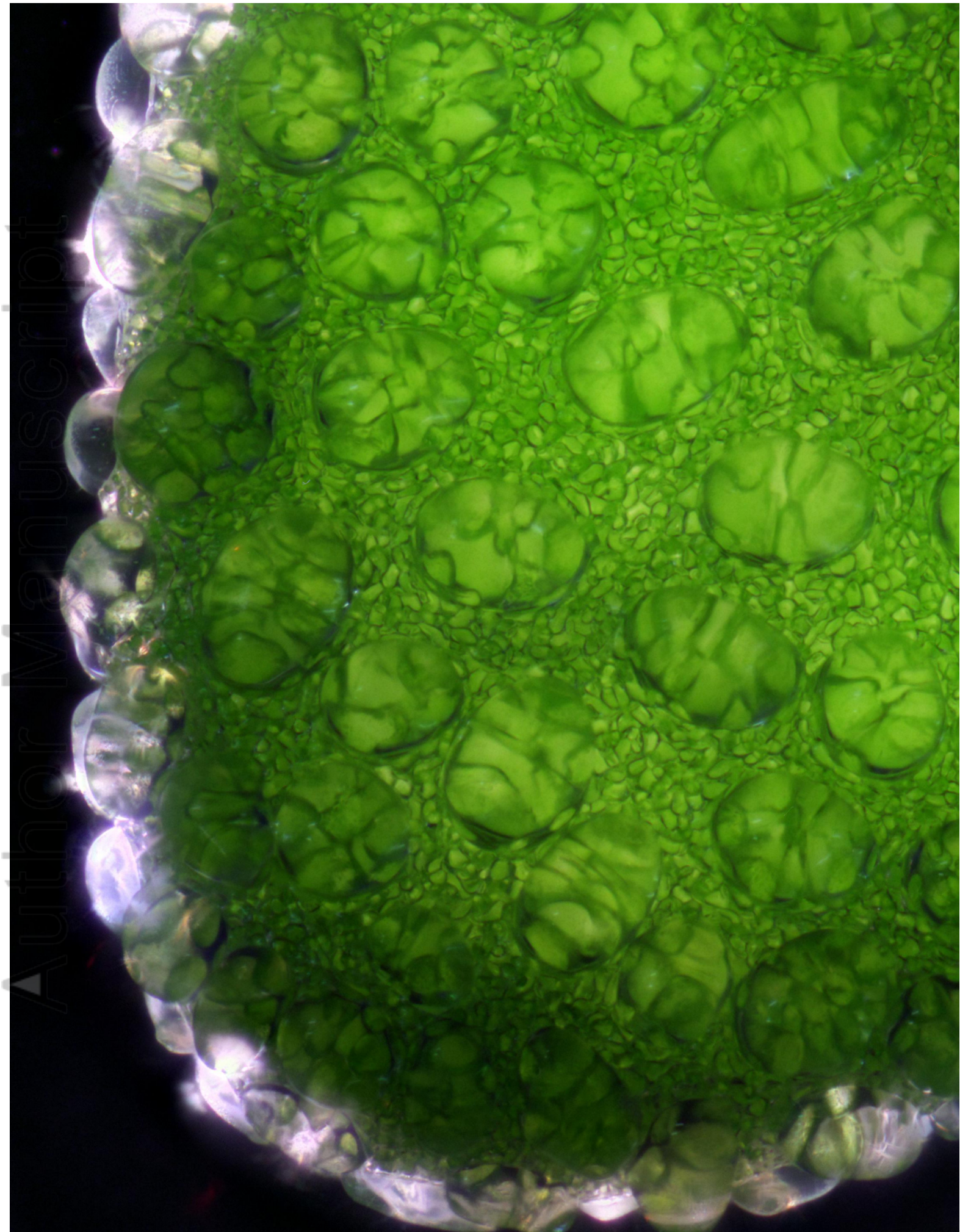
to display experimental group scores. (B) Loadings plot for the selected principal components in A.

**Supplementary Figure 3.** Important features selected by volcano plot with fold-change threshold  $> 2.0$  (x-axis) and FDR-adjusted  $p$ -value threshold  $< 0.05$  (y-axis). The pink circles represent features above the thresholds. Note both fold-changes (salt treatment relative to control) and FDR-adjusted  $p$ -values are log-transformed. The farther its position away from the (0, 0), the more significant the feature.

**Supplementary Figure 4.** PL-based signalling mechanisms in EBC are responsive to salt treatment. Overview of PIP and PA-based signalling components in EBC based on Munnik and Vermeer, (2010). The gene products involved in each metabolic step (black arrows) are shown in italics. The corresponding transcripts identified in EBC and their regulation upon salinity are indicated as follows: gray, not identified in EBC transcriptome; black, not responsive to salt treatment; red, identified in EBC and increased under salinity; and blue, identified in EBC and decreased under salinity. The corresponding  $\text{Log}_2$  (fold-change) values for statistically responsive transcripts are indicated next to them; multiple values are shown for those transcripts for which more than one homolog was identified in EBC. The changes of the overall amounts of glycerolipid classes on a per cell basis are indicated (upward red arrow: increase). Gene products: InsPase, inositol monophosphatase; MIPS, myo-inositol-3-phosphate synthase; PAK, PA kinase; PAP, PA phosphatase; PI3K, PI-3-kinase; PI4K, PI-4-kinase; PI3P, PIP 3-phosphatase; PI4P, PIP 4-phosphatase; Sac-PIP, Sac domain-containing



PIP phosphatase. Compounds: DGPP, diacylglycerolpyrophosphate; Glc6P, glucose-6-phosphate; Ins, myo-inositol; Ins3P, myo-inositol-3-phosphate; PI(3)P, PI 3-phosphate; PI(4)P, PI 4-phosphate; PI(5)P, PI 5-phosphate.



leaf tip with bladder cells.png  
This article is protected by copyright. All rights reserved.

Salinity tolerance in halophytes has primarily focused on the mechanisms for sodium accumulation and osmotic adjustment; however, sodium uptake and sequestration would require dramatic changes in the organization and dynamic properties of cell membranes as well as increase the energy requirement needs of the cell to drive the increased sodium accumulation. In this study we profiled salt-induced changes in key plant lipid species in the epidermal bladder cells of the halophyte *Mesembryanthemum crystallinum* using a targeted analysis. Our results provide new insights into the effect of salinity on lipids in plants and allows us to integrate our accumulating knowledge on the salt-induced changes in transcripts, proteins and metabolites in epidermal bladder cells with the data of cell-type-specific regulation of lipid metabolism.

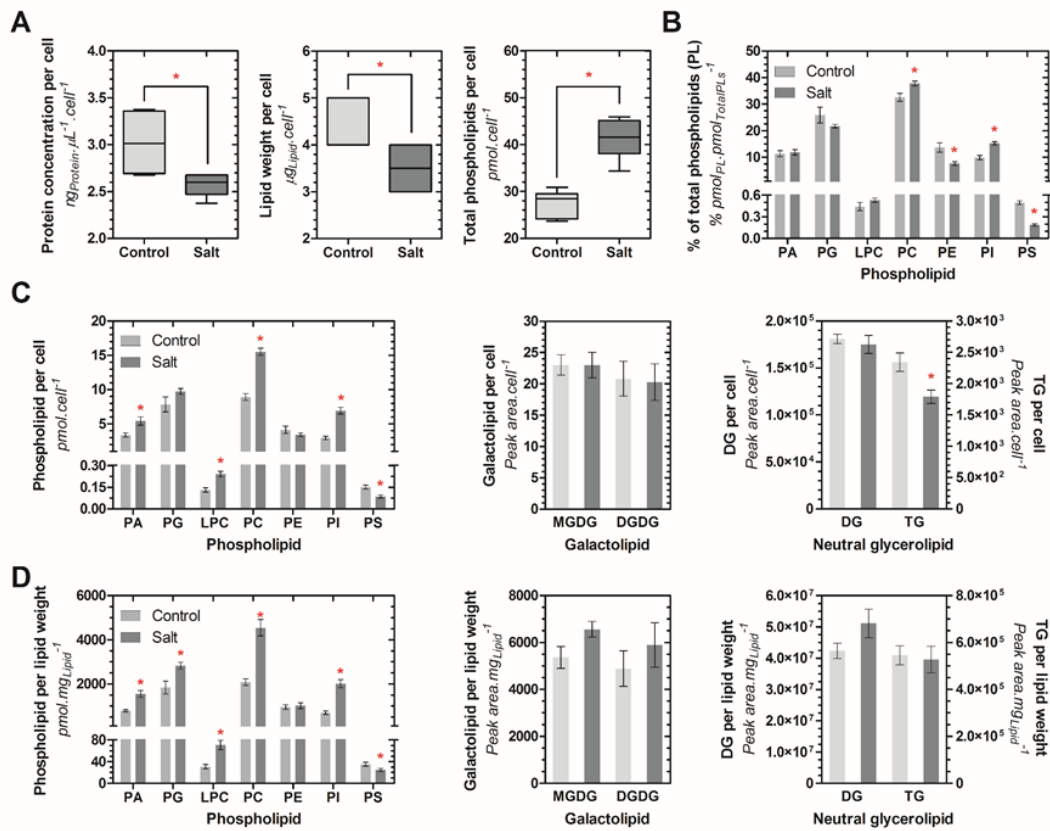


Figure 1.

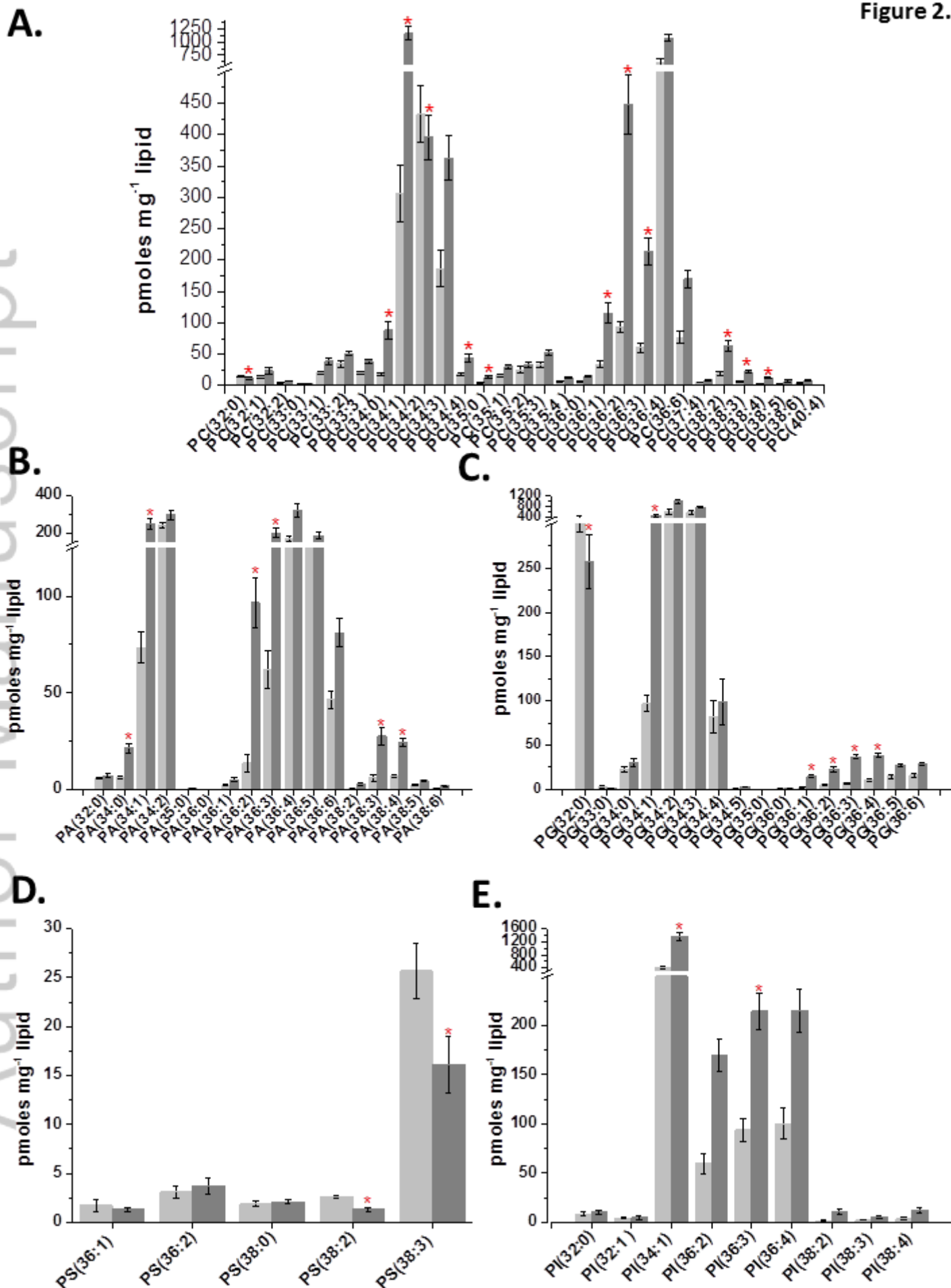


Figure 3.

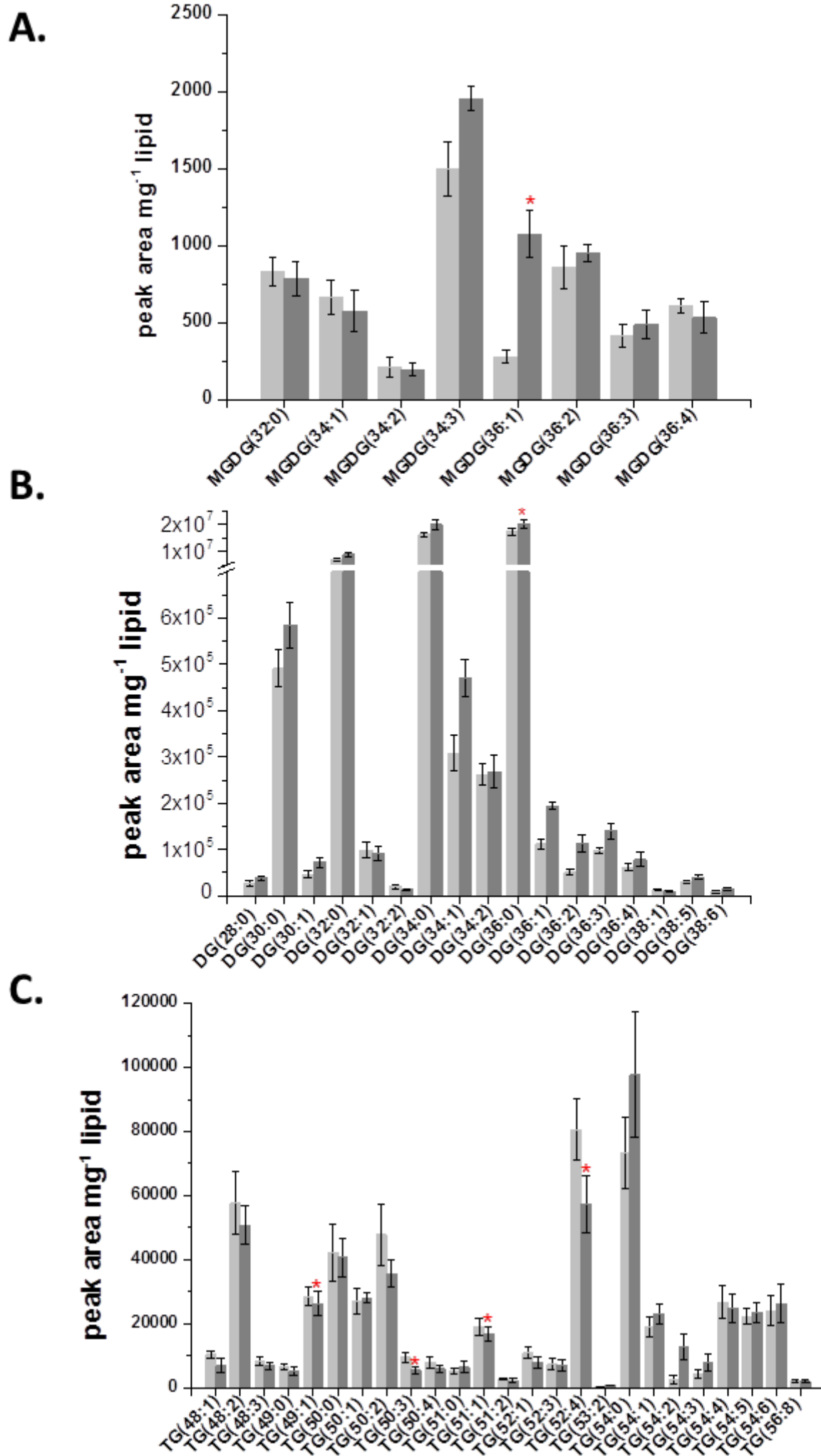
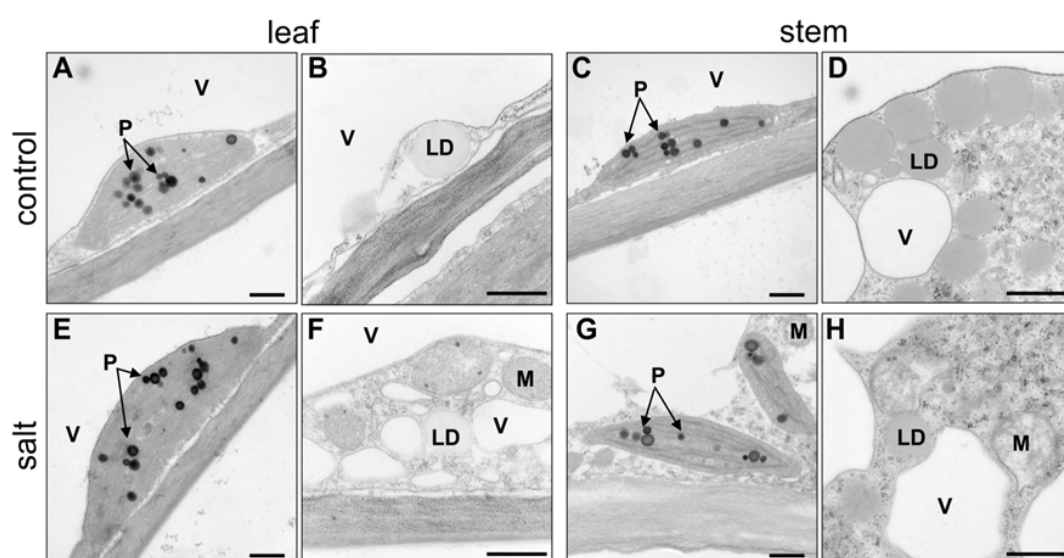
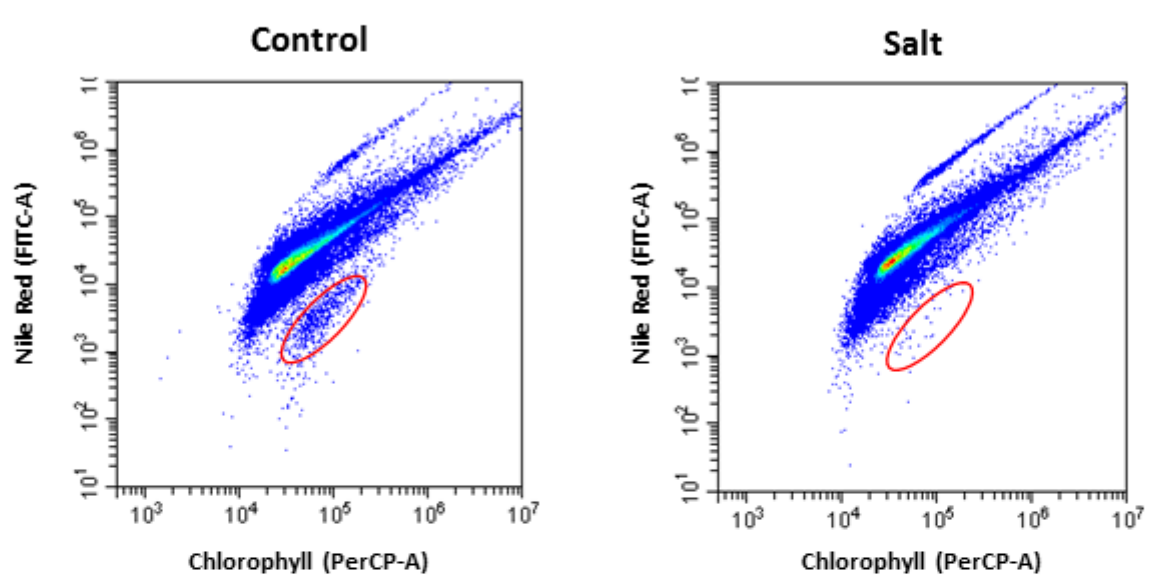


Figure 4



**A.**



**B.**

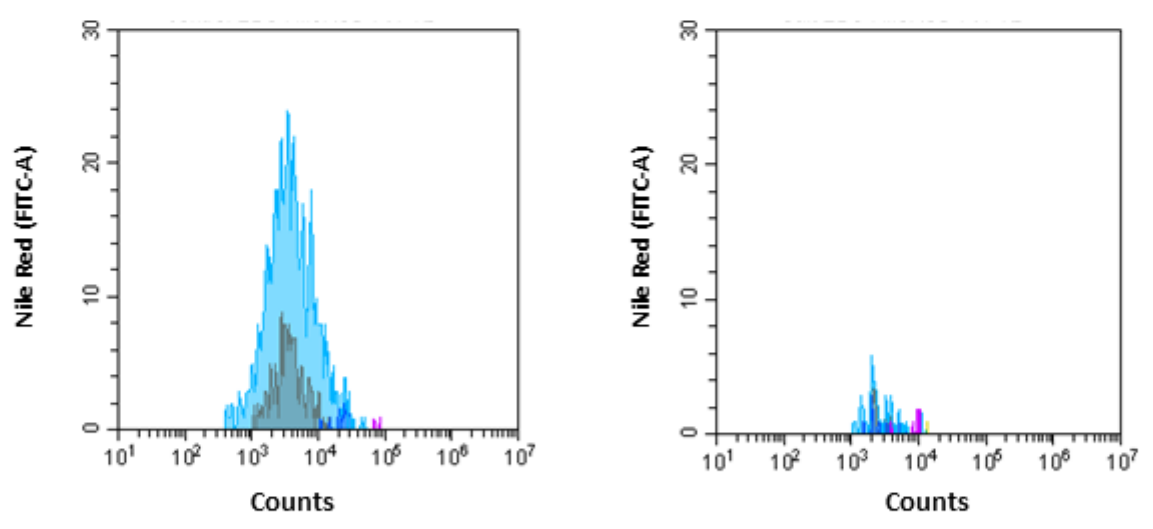
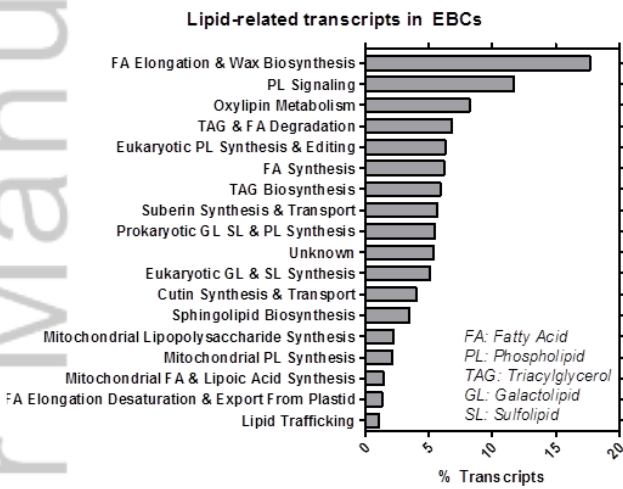




Figure 6

A.



B.

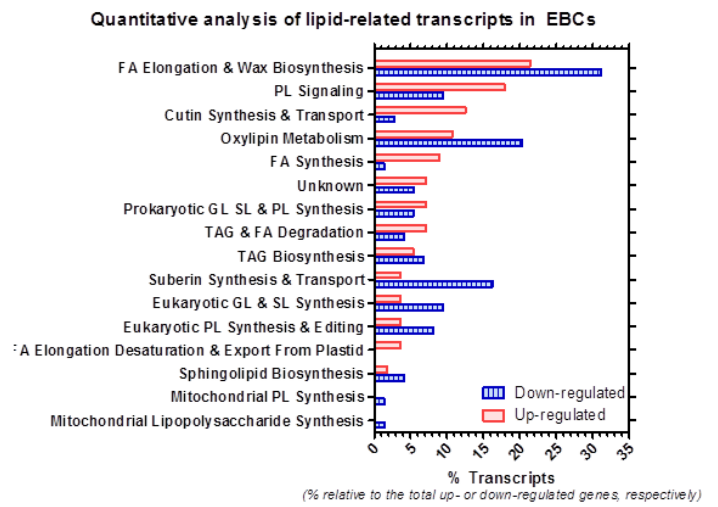
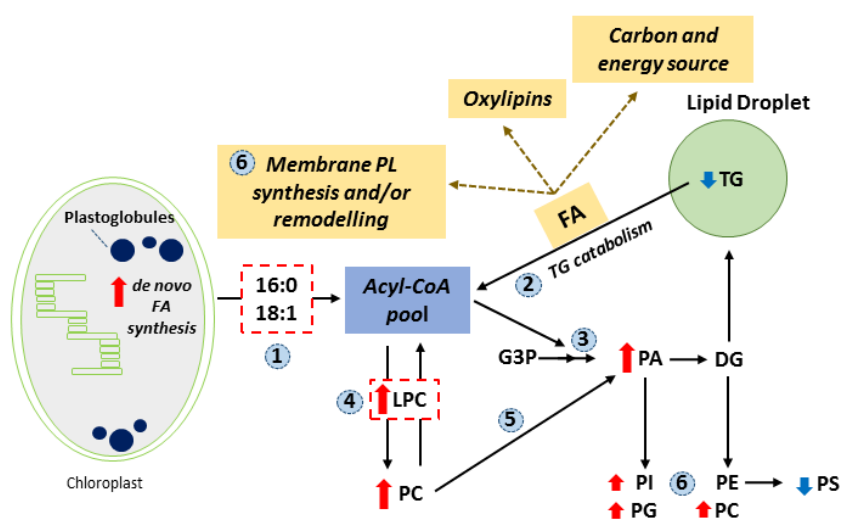


Figure 7





Minerva Access is the Institutional Repository of The University of Melbourne

**Author/s:**

Barkla, BJ; Garibay-Hernandez, A; Melzer, M; Rupasinghe, TWT; Roessner, U

**Title:**

Single cell-type analysis of cellular lipid remodelling in response to salinity in the epidermal bladder cells of the model halophyte *Mesembryanthemum crystallinum*

**Date:**

2018-10-01

**Citation:**

Barkla, B. J., Garibay-Hernandez, A., Melzer, M., Rupasinghe, T. W. T. & Roessner, U. (2018). Single cell-type analysis of cellular lipid remodelling in response to salinity in the epidermal bladder cells of the model halophyte *Mesembryanthemum crystallinum*. *PLANT CELL AND ENVIRONMENT*, 41 (10), pp.2390-2403. <https://doi.org/10.1111/pce.13352>.

**Persistent Link:**

<http://hdl.handle.net/11343/284201>

**File Description:**

Accepted version